

PROBABILISTIC SSSI ANALYSIS OF REACTOR AND AUXILIARY BUILDING WITHOUT AND WITH INCOHERENCY EFFECTS

Holger Senechal¹, Philipp Linneweber², Davide Kurmann³, Dan M. Ghiocel⁴

¹ Structural Engineer, KAE GmbH, Hausen, Germany (senechal@kae-gmbh.de)

² Structural Engineer, KAE GmbH, Hausen, Germany (linneweber@kae-gmbh.de)

³ Structural Engineer, Axpo Power AG, Baden, Switzerland (davide.kurmann@axpo.com)

⁴ Chief of Engineering, Ghiocel Predictive Technologies, Inc., New York, USA (dan.ghiocel@ghiocel-tech.com)

ABSTRACT

The objective of this paper is to compare and discuss selected result quantities from different seismic analyses for two existing nuclear structures: (a) single soil-structure-interaction (SSI) and (b) structure-soil-structure-interaction (SSSI) of two adjacent buildings. The motivation in this context is to examine whether a mutual impact of these buildings can occur during a seismic event. In addition, the paper also investigates the influence of ground-motion incoherency. Seismic result quantities are obtained with the semi-probabilistic approach implementing the Latin Hypercube Sampling (LHS) method to generate a near-random sample of 30 parameter values from a multidimensional distribution.

The existing ACS SASSI calculations of the two individual buildings (ZA, ZC) form the basis. These are merged to a common SSSI model and 30 probabilistic calculations are performed. In a further step, these 30 calculations are repeated considering incoherency for hard rock (Abrahamson, 2007). Figure 1 gives an overview of the calculations performed.

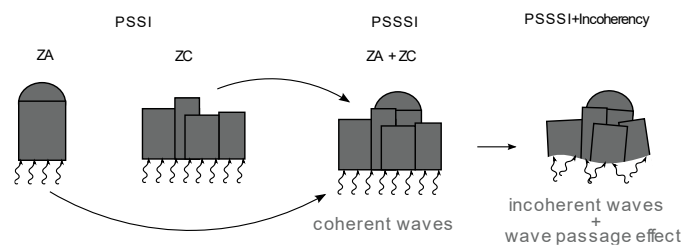


Figure 1. Variation of the probabilistic SSI and SSSI calculations.

The results of the present case study show that the effects of a more sophisticated SSSI, compared with a classical probabilistic SSI, do not affect every seismic result quantity in the same way. The effect on the probabilistic floor response spectra (FRS) due to the mutual influence of the buildings generally leads to a slight shift of the maximum spectral acceleration towards the low-frequency region. In the vertical direction, the effects of SSSI compared with single SSI in the FRS are more evident, especially for the structure with the lower structural mass. Generally, in the high-frequency range the spectral accelerations of SSSI and SSI are in good agreement. This observation also applies to the comparison of the maximum relative displacements of the two seismic analyses, even though the frequency content diverges at the levels of the nodal time histories. It could be shown that effects of incoherency on the seismic results quantities are of minor importance for the presented case study.

INTRODUCTION

In May 2016 the Swiss Nuclear Safety Inspectorate (ENSI) published – after a comprehensive review of the probabilistic seismic hazard study PEGASOS Refinement Project – the new seismic hazard provisions ENSI-2015. According to the Swiss nuclear provisions and laws, the four existing Swiss nuclear power plants (NPPs) were required to re-evaluate the seismic risk of the nuclear facilities, update their seismic probabilistic safety analysis (PSA) and carry out deterministic safety analyses (DSA) for the ENSI-2015 seismic hazard.

According to the ENSI technical note ENSI (2014) the estimation of the resulting motion quantities (FRS, seismic forces and moments, relative displacements, etc.) may be obtained by means of two approaches: classic deterministic or probabilistic (LHS) method. Guidance concerning the two methodologies may be found in KTA2201 (2011) or ASCE4-16 (2017) respectively.

THEORETICAL BACKGROUND

An earthquake is caused by the release of large amounts of energy during a shear rupture (Figure 2). Different types of waves release this energy into the environment. A probabilistic description of the complex influencing variables such as soil properties can be considered state of the art. Here, the so-called Probabilistic Soil Structure Interaction (PSSI) is presented. It is extended by considering another building nearby (PSSSI) and including incoherency effects.

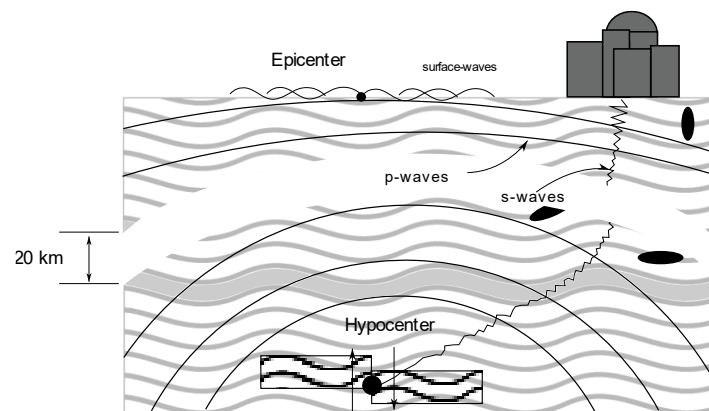


Figure 2. Schematic representation of earthquake waves (P,S,R) in the ground.

Probabilistic Soil-Structure Interaction (PSSI)

In the probabilistic approach according to ASCE4-16 (2017)¹, all relevant parameters (excitation, soil properties, building properties) of the soil-structure interaction are varied and calculated in several computational runs with these scattered parameters. As one of the precursor in the field, the US standard for safety-related nuclear structures, ASCE4-16 (2017), provides technical guidance for the systematic execution of probabilistic seismic soil-structure-interaction analyses to obtain the probability distribution of seismic responses of interest. In the present case, 30 seismic calculations are performed with software code ACS SASSI Ghiocel Predictive Technologies (2022). The excitation is varied using the acceleration time histories of recorded strong earthquakes (seeds). These are iteratively matched to the specified free-field spectra (matches), for obtaining site-specific spectra-compatible earthquake time histories but their peak-to-

¹ Please note, that in contrast to ASCE4-16 (2017), where 80% non-exceedance-probability (NEP) is suggested, the 84% NEP is used for subsequent analyses of SSC, as requested by ENSI.

valley variability as well as the component-to-component variability in the horizontal directions of motion are preserved. For the variation of soil and building parameters, the respective best-estimate values are scattered using Latin hypercube sampling (LHS), hence providing stochastic sets of model properties each together with a randomly chosen excitation. The evaluation of the individual ACS SASSI calculations is then also performed using statistical tools assuming a log-normal distribution of the seismic responses of interest. The median value for the PSA and the 84th percentile for the DSA is evaluated from the individual results.

Structure-soil-structure interaction (SSSI)

In ACS-SASSI the dynamic soil-structure interaction, the mutual influence of building and soil is calculated in the frequency domain. Today's practice in nuclear industry considers, that the building in question is located at the free field and that this free field - i.e., the soil - is homogeneous in each layer and the influence of adjacent structures on the seismic responses may be neglected. Among this, it should be pointed out, that in the past decades, such computationally intensive SSI problems could only be calculated at all by simplifications. In many cases, these simplifications are permissible, but interfering factors like e.g.

- a large or heavy structure in the immediate vicinity,
- a ravine or a deep crevice in the ground,
- or a strongly inhomogeneous or not horizontally layered soil

require the use of detailed analyses (i.e., SSSI models). In this case, the disturbance factor (e.g., a tunnel, a large neighboring building, an inhomogeneous soil confinement...) above or in the soil is also modeled in the computational model and thus the interaction between disturbance factor, soil and structure is considered.

Modelling of incoherency effects

Usually, in a SASSI calculation, the assumption is made that the earthquake waves, generated by the tectonics of continental plates, are coherent (equal in frequency and phase) at the point of action per soil layer. Therefore, the ground can be modeled in a simplified way as a one-dimensional column. In the nuclear industry, shear waves acting vertically in the X-direction (SV), shear waves acting horizontally in the Y-direction (SH), and compression waves acting in the Z-direction (P) are assumed to be the loading magnitudes (ASCE practice). However, two aspects can lead to the fact that the coherence of the earthquake waves at the point of action is no longer given:

- Wave Passage Effect: Depending on the dimensions of the structure and the ground stiffness or shear wave velocity, phase shifts occur as a result of different travel times of the shear waves at opposite edges when passing the foundation (Figure 3).
- Wave Scattering Effect: As a result of disturbances in the upper 500 m of the soil, there is a scattering of the shear waves. The greater the variability of the soil layers in the horizontal direction, the greater this scattering or incoherency. Topographic features (e.g., inclination of the soil layers) are also important. The distance between two considered points on the surface (separation distance) and the frequency are the main influence parameters of the incoherency.

Earthquakes usually occur at a depth of 10 km to 50 km. The shear wave velocity is more or less high in the ground and only decreases in the last 200 m to 500 m - the shear waves are considerably decelerated. Figure 3 shows an example of an earthquake area and the vs ground profile in the upper 1000 m of ground. Because of this sharp decrease in shear wave velocity, inhomogeneities in the ground are of particular importance to incoherency, especially in the upper ground region. In general, the source (point/line) does not affect the incoherency of two neighboring points at the target due to the large distance (see Figure 3). However, especially in the case of strong, nearby earthquakes, the incoherency of the waves at the target may be amplified.

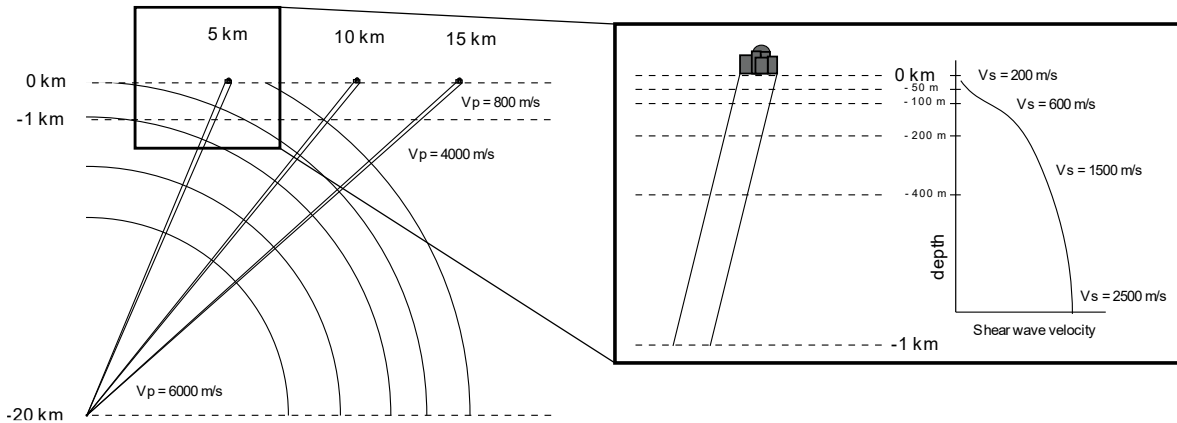


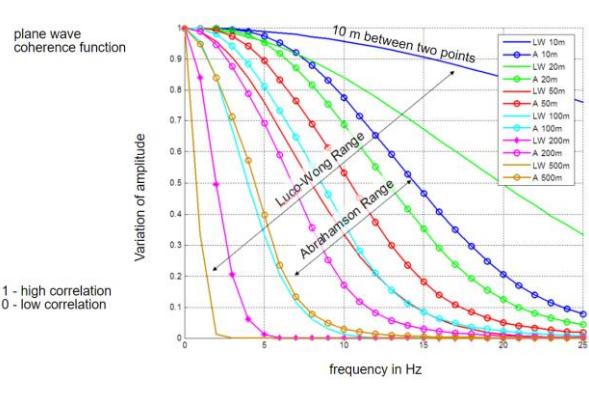
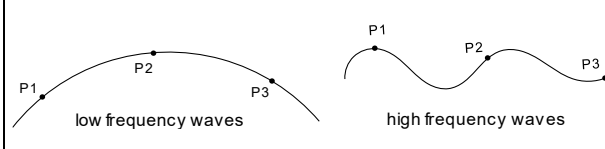
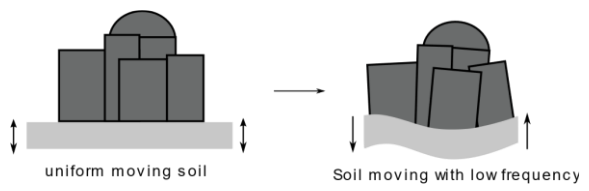
Figure 3. Illustration of an earthquake with the shear wave velocity profile.

All causes of wave scattering are difficult to detect without measurement of actual earthquakes since this requires knowledge of the point of origin or the direction of propagation as well as a detailed image of the ground including local faults in the near field of the considered location (up to max. 500 m depth). Furthermore, calculations with physical models according to Abrahamson lead to an overestimation of the incoherency for small distances. Therefore, it is more advantageous to consider the incoherency by probabilistic approaches. Abrahamson has done extensive research on this, summarized in Abrahamson (2007), and developed appropriate coherence curves for probabilistic calculations. Application of these are a good compromise compared to the effort that would be required to determine site-specific coherence functions.

The ideas underlying the mathematical equations of incoherency are briefly summarized in Table 1. A more comprehensive introduction can be found, for example, in Ghiocel et al. (2017).

Table 1. Brief mathematical introduction of modelling incoherency effects.

Mathematical description	
<p>The seismic spatially varying stochastic field S_{U_j,U_k} is described as a space-time stochastic process with a Gaussian probability distribution (Equation 1). It is computed by taking the power-spectral density description S w.r.t. two soil locations j, k times the coherence function of those points:</p> $S_{U_j,U_k} = \underbrace{\left[S_{U_j,U_j}(\omega) S_{U_k,U_k}(\omega) \right]^{1/2}}_{\text{local random variation}} \cdot \underbrace{\Gamma_{U_j,U_k}(\omega)}_{\text{coherence function}} \quad (1)$	
local random variation	
	<p>The seismic load vector is varied with respect to direction and magnitude using a stochastic approach (e.g., Monte Carlo) as shown in Figure 4. In this way, inhomogeneities in the soil (e.g. faults, variation in soil layers) are mapped.</p>
<p>Figure 4. Variation of the seismic load vector.</p>	

coherence function	
<p>The coherence function (Equation 2) is computed by the plane wave coherence and (optional) times the wave passage function:</p> $\Gamma_{U_j, U_k}(\omega) = \underbrace{\Gamma_{PWU_j, U_k}(\omega)}_{\text{plane wave coherence}} \underbrace{\exp[i\omega(X_{D,j} - X_{D,k}/V_D)]}_{\text{wave passage fct.}} \quad (2)$	
plane wave coherence	
 <p>Figure 5. Coherence functions. extracted from Ghiocel et al. (2007).</p>	<p>The plane wave coherence functions (depicted in Figure 5) describe the influence of two points onto each other. Two points close to each other show a strong correlation of the amplitude over the entire frequency range. Points far away show high correlations only at low frequencies (Figure 6).</p>  <p>Figure 6. Sketch concerning the variation of points as a function of the wave frequency.</p>
wave passage function	
 <p>Figure 7. Wave passage effect.</p>	<p>Depending on the dimensions of the structure and the soil stiffness or shear wave velocity, phase shifts occur due to different travel times of the shear waves at opposite edges when passing the foundation (compare Figure 7).</p>

MODEL DESCRIPTION

Building model

The present case study aims to estimate the relative movements between the reactor building (ZA) and the auxiliary building complex (ZC) of the Leibstadt NPP by merging the two existing model and performing a probabilistic SSSI. In the process, the two soil models, in particular the layer thicknesses, are also aligned and combined into a single soil model. Due to the surrounding buildings, embedment is only considered from -10 m.

The ZA building has a circular shape with a diameter of about 42 m and is shallowly founded at -9.8 m (Figure 8 a). The ZC building complex (Figure 8 b) is a collection of different interconnected buildings of varying depths with a more or less rectangular shape. The exterior dimensions are approximately

74 m x 54 m. In the center there is a circular recess into which the reactor building is inserted. The foundation is deeper than -10 m only in the northern area, where it is modeled as embedded (Figure 8 c). The two buildings are not structurally connected and have a distance of at least 50 mm from each other.

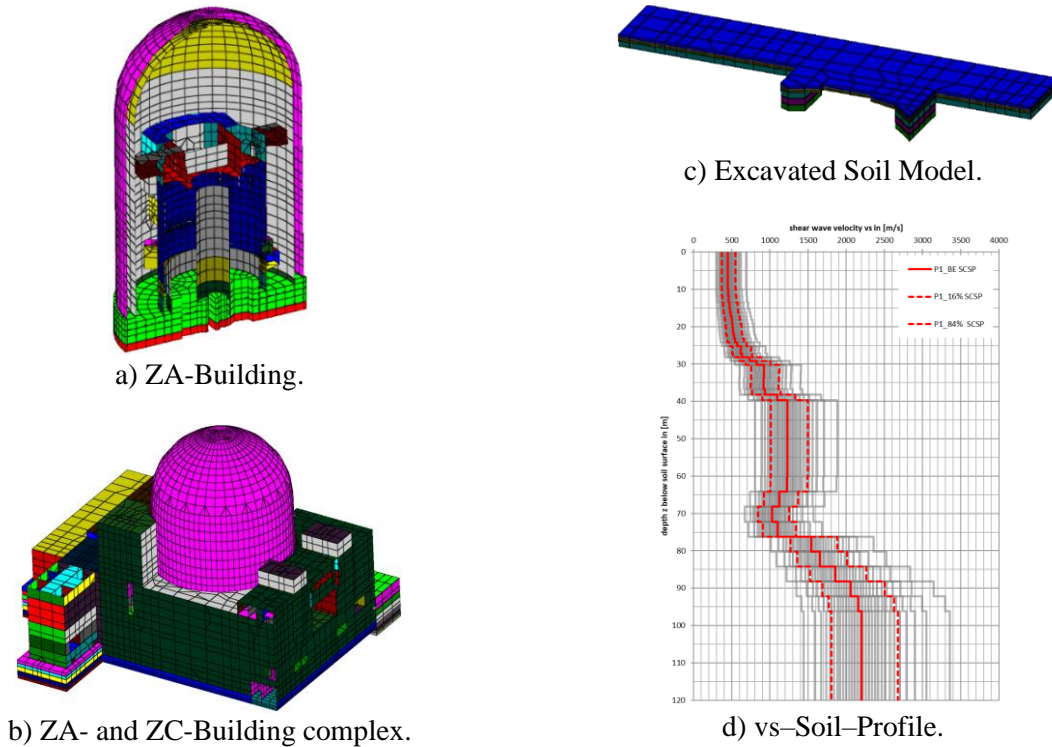


Figure 8. SSSI building model.

Soil model

For the soil model (Figure 8 d) the properties (stiffness, damping) from extensive soil investigations carried out at the site over the past decades were applied. The geological conditions in the immediate vicinity of the site were used to create the best estimate soil model. In addition, strain-compatible soil properties are calculated utilizing the defined free-field spectra.

Latin Hypercube Sampling Multipliers

In the framework of the probabilistic SSI analysis the following variables, that governs the overall system response, have been selected for generating Latin Hypercube Sampling (LHS):

- soil shear wave velocity (profile),
- soil material damping (profile),
- structural Young's modulus E of concrete (or steel) and
- structural material damping ratio of concrete.

According to the common practice and the minimum requirements in US standard ASCE4-16 (2017) a total of 30 intervals have been defined for the scope. This implies, that a total of 30 SASSI Input-Models will be generated to estimate the statistical distribution of the different results quantities arising from the probabilistic SSI analysis of each structure. The LHS is a statistical method for generating a near-random sample of parameter values from a multidimensional distribution. The sampling method is used in

the framework of this project to generate a representative sampling of N variables divided into M intervals. When sampling a function of N variables, the range of each variable is divided into M equally probable intervals. M sample points are then placed to satisfy the Latin hypercube requirements. Note that:

- this forces the number of divisions M to be equal for each variable,
- this sampling scheme does not require more samples for more dimensions (variables).

The latter point (independence) is one of the main advantages of this sampling scheme. Another advantage is that random samples can be taken one at a time, remembering which samples were taken so far. The single variables have been assumed to be log-normal distributed. In statistics the term cross-correlation is used for referring to the correlations between entries of two random vectors X and Y. The definition of correlation always includes a standardizing factor in such a way that correlations have values between -1 and +1. The logarithmic standard deviations (beta) for the variables 1 to 4 were set equal to:

- variable 1 $\beta = 0.199$ and COV = 0.20,
- variable 2 $\beta = 0.340$ and COV = 0.35,
- variable 3 $\beta = 0.294$ and COV = 0.30,
- variable 4 $\beta = 0.340$ and COV = 0.35.

The results of the LHS multipliers are documented in Table 2. The multipliers lead to an acceptable range of the effective (real) values for the four parameters. The ensemble of the developed 30 shear wave velocity and soil damping profiles (strain compatible level) are then obtained by multiplying the property values with their corresponding LHS multiplier.

Table 2. Latin hypercube sampling (LHS) parameters.

COV (input)	0.2	0.35	0.3	0.35
Case no.	Soil vs. Layer	Soil damping	E-Modulus structure	Structure damping
1	1.1	0.51	0.82	0.64
...
30	0.99	1.18	0.53	1.16
Min	0.65	0.48	0.53	0.52
Max	1.53	1.86	1.87	1.59

Incoherency parameters

For incoherency, the 2007 Abrahamson model is used for hard rock sites. The wave propagation is isotropic (in ACS SASSI 0° radial angle to the X-axis). As mentioned previously, the addition of incoherency in the LHS procedure does not increase the number of samples. It merely adds another column of incoherency to Table 2. The Python scripts used to create and compute the 30-input sets and post-processing can be reused from the coherent SSSI calculation.

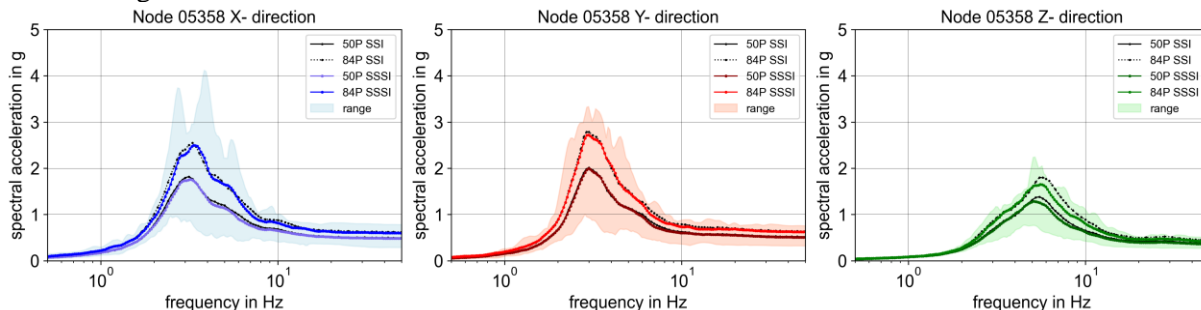
RESULTS

Figure 1 provides an overview of the calculations performed. The results of the individual calculations are presented and compared with each other. In addition to the determination of the relative displacements for the evaluation of a possible impact, the floor response spectra are compared with each other. Generally, the 50% resp. 84% non-exceedance probability (NEP) level of the seismic response of interest has been selected for the scope because of the implications in a PSA and classical DSA.

Comparison of the response spectra of SSI and SSSI

Figure 9 and Figure 10 show the 50% and 84% non-exceedance-probability (NEP) of selected FRS (5% critical damping) resulting from probabilistic SSI (black lines) and SSSI (colored lines) as well as the range of the 30 single SSSI occurrences. Figure 9 shows the results close to the ground surface while Figure 10 depicts the FRS at almost 15m above ground level.

ZC-Building



ZA-Building

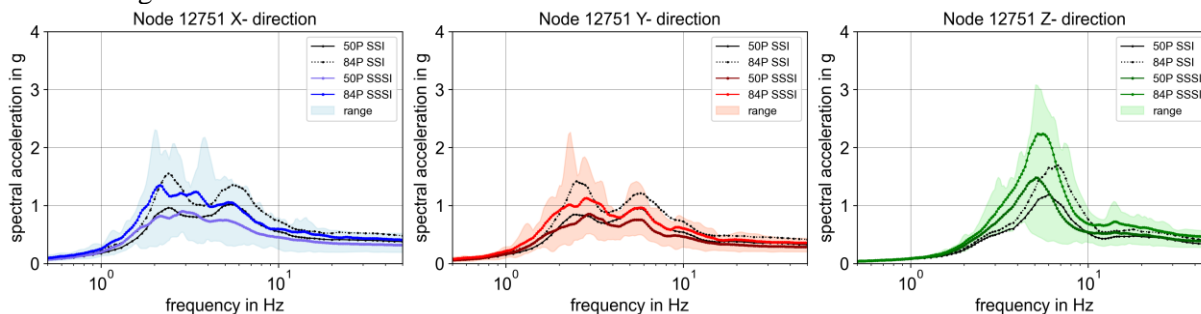
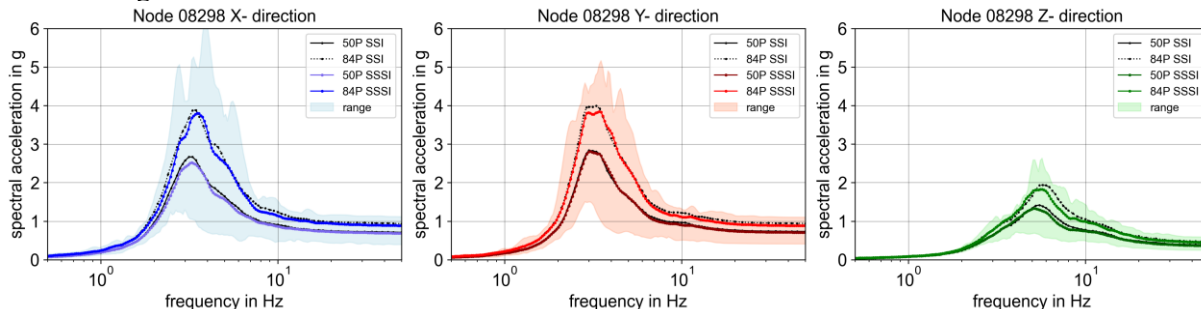


Figure 9. FRS at ground level, a) ZC building -2.5m, b) ZA building +3.2m.

With respect to the SSI of a single structure as well as a shift of the spectral acceleration peaks toward lower frequencies in the three spatial directions of motion, (particularly for the 84% NEP). In both horizontal direction the maximum spectral value is almost unaffected in SSSI or even lower when compared with SSI. In contrast, we observe the most significant divergences between SSI and SSSI in the vertical direction of motion. Especially for the enclosed ZA building, the vertical response is influenced by the surrounding ZC structure, which exhibits the greater structural mass. It should be noted that the above considerations are specific to the present case study. Extrapolation to other dynamic systems should be carefully considered.

ZC-Building



ZA-Building

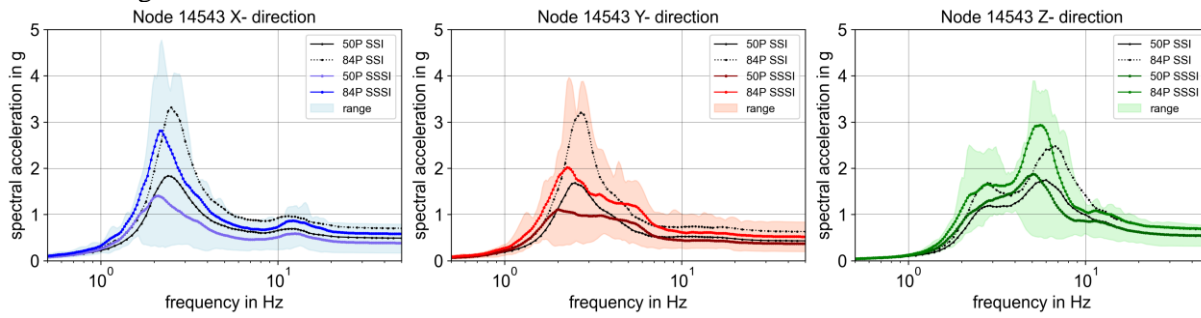


Figure 10. FRS at high level, a) ZC building 16.2 m, b) ZA building 15.3 m.

From the above images, it can be observed that the SSSI mainly affects the spectra of the ZA when compared to ZC building. Compared to the stand-alone SSI calculations, the SSSI model partially gives different results independent of the SSI calculations. The mutual influence in the SSSI calculation is complex and no general statement on the validity of SSI calculations can be made from it. Due to the larger oscillating mass and the larger number of substructures, and thus natural frequencies.

Comparison of the spectra of SSSI without and with incoherency

Figure 11 shows the influence of incoherency in the SSSI calculation. Again, a node near the ground and a node at high altitude are selected. It is to be noted that at both altitudes only minor influences of incoherency are shown in the response spectra. At the same time, no tendency of reduction or exaggeration can be observed in the very similar curve shape. The presented conclusion may not be representative in a general manner and different incoherency models and dynamic characteristic of the structural systems may lead to other conclusions.

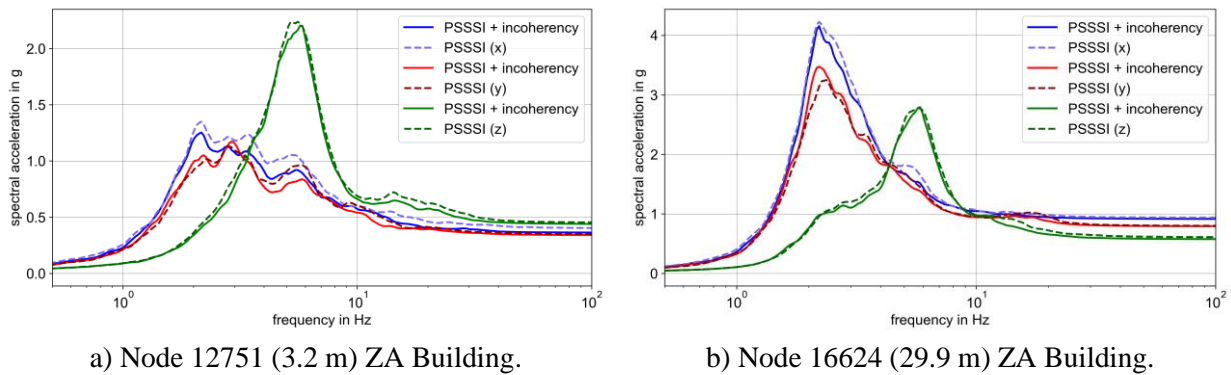


Figure 11. FRS from PSSSI.

Relative displacement between reactor and auxiliary building

For the determination of the relative movements between ZA and ZC, two adjacent building nodes are considered at approx. 21.5m. From the SSI calculations the 84% NEP maximum relative displacements (absolute values over time) are retained and combined with the SRSS method. A horizontal relative movement of 52 mm results (nominal building gap measure 50-100 mm). According to this preliminary evaluation, further considerations are necessary.

For the evaluation of a mutual impact of the two buildings due to earthquake movements, the radial relative movements of the two nodes mentioned above (8996-ZC, 15459-ZA) are extracted. The SSSI calculation results in a 84% NEP value of 39.9 mm (compared to 36.6 mm for SSSI+Incoherency) as the maximum displacement with respect to each other. The 84% NEP value was determined from the respective displacement maxima of the 30 calculations. Therefore, an impact of the buildings is impossible.

Figure 12 depicts the gap opening distance over time. An initial opening of 50 mm is generally assumed for all the dynamic analyses.

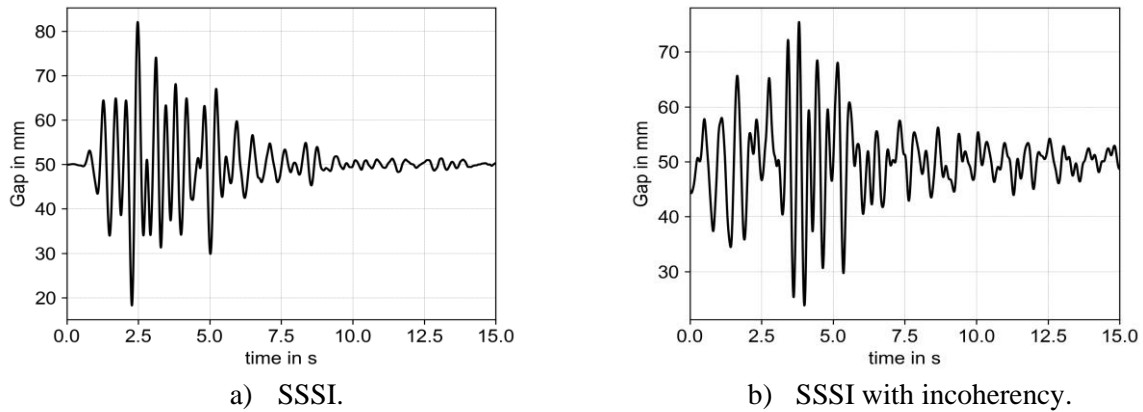


Figure 12. Resultant gap between neighbored ZC- and ZA-nodes for Match 7.

Although the resulting gap magnitude between SSSI and SSSI + incoherency is very similar, Figure 13 b) depicts large-wave low-frequency seismic waves, which do not occur in figure a). Thus, an effect of incoherency is clearly visible. It results from low frequency wave propagation, which is accounted for in the incoherent variant, while the ground moves uniformly up and down as a rigid unit in the coherent variant. Since the resulting displacement is relative to the moving ground, the uniformly moving soil filters the low frequency waves (compare Figure 7). In addition it should be noted that, because of the random phase shifting approach in the incoherent calculations, the initial gap distance isn't 50 mm.

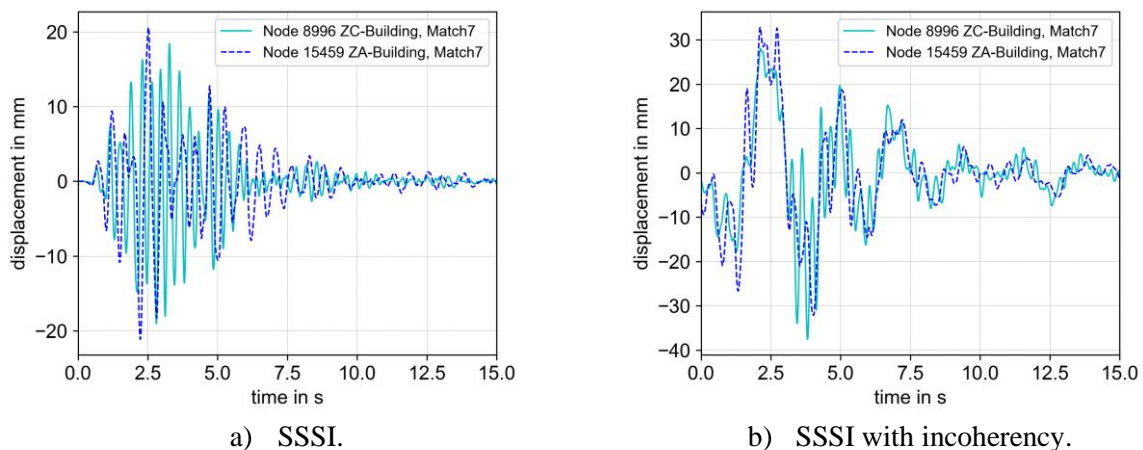


Figure 13. Time history displacement of neighbored ZC and ZA nodes.

CONCLUSION

An extensive case study investigated the effects of SSSI and incoherency on selected seismic responses for two existing nuclear structures on the Swiss NPP-Site of Leibstadt. For the scope, probabilistic seismic analyses in ACS SASSI were performed. The results of the case study show, that the SSSI frequently exhibits slightly around the maximum spectral acceleration compared to SSI (especially for 84% NEP), because of the large number of substructures and interferences between the oscillating masses. SSSI also exhibits a FRS shifting toward lower frequencies that may be associated with a de- or amplification of the maximum spectral values compared with SSI. Because the seismic capacity of systems, structures and components (SSC) typically depends on the interaction of the three spatial directions, local FRS divergences between SSI and SSSI for single frequency ranges or directions are typically of minor impacts on SSC fragilities.

Zero-Period accelerations (ZPA) in FRS usually correlates with resulting seismic forces and moments of buildings; for the case study it seems that ZPA are almost unaffected to SSSI when compared to SSI. The last comment is still valid for incoherency effects even though the resulting nodal time-histories are significantly different in terms of frequency content when compared with a coherent analysis. As expected, the explicitly considered gap width between the buildings reacts particularly sensitively to the consideration in an SSSI model and the resulting relative displacements are reduced. This evidence may be of importance when analyzing mechanical systems (e.g., pipe calculations) and the seismic displacement-induced stresses leading to unnecessary retrofitting projects.

Summarized, the comparative results of probabilistic SSI and SSSI for two safety-related nuclear structures can help to provide a better understanding of the magnitude and uncertainties associated with SSI analyses of single structures.

REFERENCES

- Abrahamson, N. (2007), *Program on Technology Innovation: Effects of Spatial Incoherence on Seismic Ground Motions*, EPRI, Palo Alto, CA:2007. 1015110
- American Society of Civil Engineers (2017), *Seismic Analysis for Safety-Related Nuclear Structures and Commentary*, ASCE4-16 Standard
- ENSI (2015), *Review Approach and Comments Concerning the PEGASOS Refinement Project (PRP) and the PRP Summary Report*, ENSI Final Report
- ENSI (2014), *Methodik deterministischer Nachweise der Schweizer Kernkraftwerke für Erdbeben der Störfallkategorien 2 und 3*, ENSI-AN-8567
- Ghiocel, D. M., Ostadan F. (2007), *Seismic Ground Motion Incoherency Effects on Soil-Structure Interaction Response of NPP Building Structures*, Transactions, SMiRT 19, Toronto
- Ghiocel, D. M. (2015). *Seismic motion incoherency effects on Soil-Structure-Interaction (SSI) and Structure-Soil-Structure-Interaction (SSSI) of different Structures for different Soil Site Conditions*, Transactions, SMiRT23, Division V, Manchester, United Kingdom.
- Ghiocel, D. M., Jang, Y. S., Lee, I. H. (2017), *Understanding Seismic motion incoherency Modelling and Effects on SSI and SSSI Responses of Nuclear Structures*, Transactions, SMiRT24, Division V, Busan, Korea
- Ghiocel Predictive Technologies, Inc. (2022). *ACS SASSI NQA - An Advanced Computational Software for 3D Dynamic Analyses Including SSI Effects*, ACS SASSI Version 4 User Manuals, Rochester, New York
- KTA 2201 (2011), *Safety Standards of the Nuclear Safety Standards Commission: Design of Nuclear Power Plants against Seismic Part 1-3*, KTA